Simulation of the hobbing process of enveloping wormwheels for the calculation of contact pattern and contact lines

Christian Kirchhoff[1], Linda Becker[1], Peter Tenberge[1]
Ruhr-University Bochum, Germany[1]
E-mail: Christian.Kirchhoff@rub.de, Linda.Becker@rub.de, Peter.Tenberge@rub.de

Abstract: *The contact pattern and contact line calculation is an essential part of the design of worm gears. The existing calculation algorithms are based on the law of gearing. For this reason, cases like meshing interferences can only be analysed to a limited extent. The simulation of the hobbing process of enveloping wormwheels, introduced here, makes it possible to generate any wheel flank precisely. For the contact pattern calculation, one wheel flank is generated from the cutter geometry and one from the worm geometry. These two generated flanks are brought into contact. For each flank coordinate, the distance to the opposite flank is obtained. The graphical application of this distance over the wheel coordinates results in a contour diagram that is known as the contact pattern. The contact line calculation of worm gears also shows on which part of the flanks power is transmitted at a certain rotational position. For this calculation, the wheel flank generated from the cutter is brought into contact with the worm flank at any angular positions.*
Keywords*: WORM GEARS, ENVELOPING WHEEL, HOBBING PROCESS, CONTACT PATTERN, CONTACT LINES*

1. Introduction

Worm gear units allow high gear ratios in one gear stage and therefore require less mounting space than other gear units that deliver the same gear ratio. Compared to spur gears, they are less efficient due to the high sliding movements, but there are applications in which this is actually an advantage. A good example are worm gear units for elevators. Here, the worm gearing can be designed to be self-locking. This helpfully causes the elevator to move only by the drive of the motor on the worm side and not by the output torque resulting from the weight of the passengers. An additional brake can be avoided in this case. Another positive feature of worm gear units is the high possible overlap of the teeth, which results in very smooth running.

The line contact between the worm and the enveloping wheel requires them to be matched very precisely with each other. The wheel is usually made of centrifugal casting bronze. This shows a good run-in behavior. It means that production-related gear deviations or drive-related deformations with initially high wear can be compensated. During the run-in phase, the wheel flank adapts to the worm geometry and the efficiency improves.

The run-in behavior can be optimized by varying the gear and manufacturing parameters. Small deviations between the worm and cutter geometry prove to be effective. Theoretically congruent flank geometries cannot be paired congruently in real terms, resulting in large wear.

To check the mounting situation of the two gears, a contact pattern test is applied by brushing the wheel flanks and then spinning the gears under load. The basic idea is that the contact pattern should not extend over the entire wheel flank in order to avoid root and edge supports as a result of deformation. However, when noise behavior is a high requirement, the contact pattern is positioned over a relatively large area and towards the root of the tooth (Fig. 1, left). The contact pattern for worm gears exposed to impact and high loads is smaller and positioned toward the tooth tip (Fig. 1, right). [1]

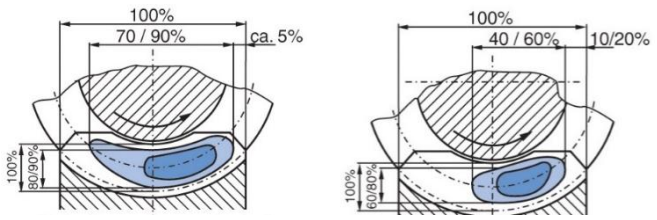

Fig. 1 *Ideal contact patterns for low-noise (left) and highly stressed gearings (right) [1]*

For gearings that are operated in both directions of rotation, the contact pattern is oriented centrally on the gear flank. If the gear unit is used primarily for one direction of rotation, the contact pattern is shifted to the run-out side. This favors the lubricant film buildup and increases the efficiency. In Figure 1, the inlet side is on the left and the outlet side on the right for both gears. [1]

2. Prerequisites and means for solving the problem

The previous section shows that the load profile calculation is an essential part of the design and manufacture of worm gears. In order to save costs and time in the production of a good contact pattern for a specific application, there still exists different software tools that calculates the contact pattern in advance with defined flanks and tool geometry. These programs are based on the law of gearing. The enveloping gear flank contour is determined analytically by the tooth contact to the worm flank. This purely analytical approach leads to problems in critical cases like meshing interferences. Likewise, the calculation of special gears such as worms with a large number of teeth or worms with a very small center pitch angle is not possible.

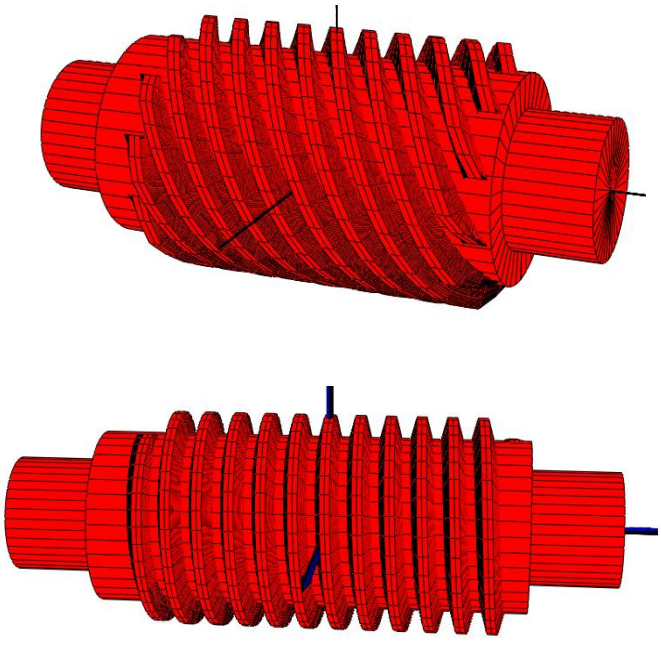

Fig. 2 *Worm with a high number of teeth (left) and with one tooth and a small pitch angle (right)*

3. Solution of the examined problem

To calculate the contact pattern and contact line of any worm gear, a numerical approach is chosen which is presented in the following. The hobbing process of the enveloping gear flank from the tool contour is simulated. This simulation uses a modification of the algorithm already successfully used for spur gears [2]. A surface element is being specified on the wheel blank, which includes the surface within the pitch angle of the wheel. This surface element is defined with two grid boundary functions. One function is located at the tooth tip (Fig.3, black) and one at the tooth root (Fig. 3, green). A certain number of points (Fig.3: 30 points) is defined on both functions. The connections between the respective opposite points of the grid boundaries are made of straight lines (Fig.3, gray), which pass through the volume element as a grid.

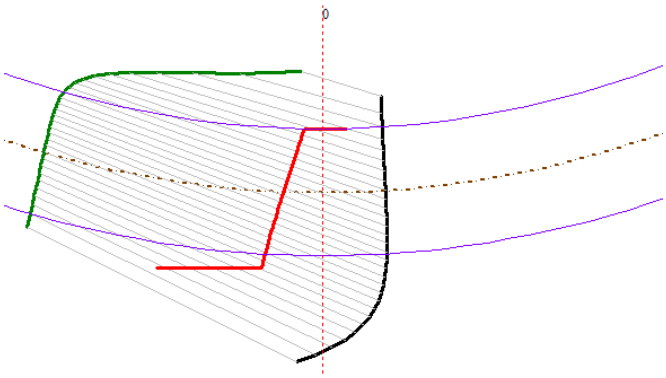

Fig. 3 *Cutter contour and surface element on the wheel blank at pitch position 0°*

This grid is rotated around the wheel axis depending on the position of the cutter geometry, so that the kinematics between the wheel blank and the tool of the hobbing process are correctly reflected. For each grid line, it can be determined in a specific rotational position if and where there is an intersection with the cutter contour. The grid is rotated from the central rotational position (Fig. 3) first to the right and then to the left until no new intersection points are found between the cutter contour and the grid lines that are closer to the tooth root boundary function (green).

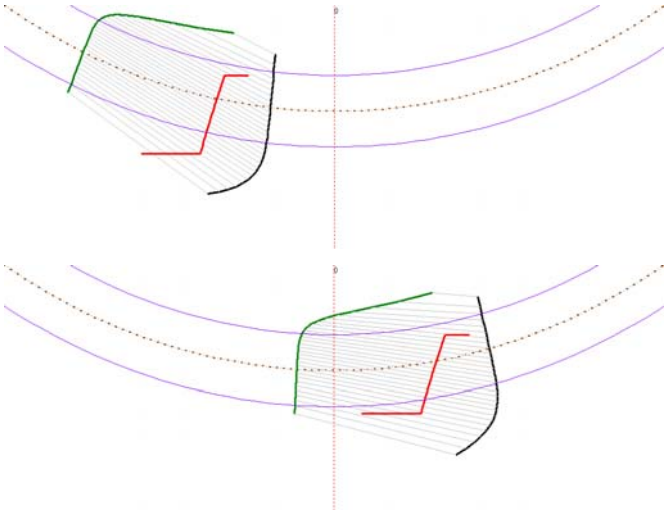

Fig. 4 *Cutter contour and surface element on the wheel blank at -9° (top) and pitch position 11° (bottom)*

During rotation in one direction, the intersection point of each grid line that is closest to the tooth root boundary function is saved from all rotation positions. The connection of all these saved points per grid line, provides the hobbed wheel contour. Any material of the wheel blank that is below these intersection points is removed in the hobbing process. [2]

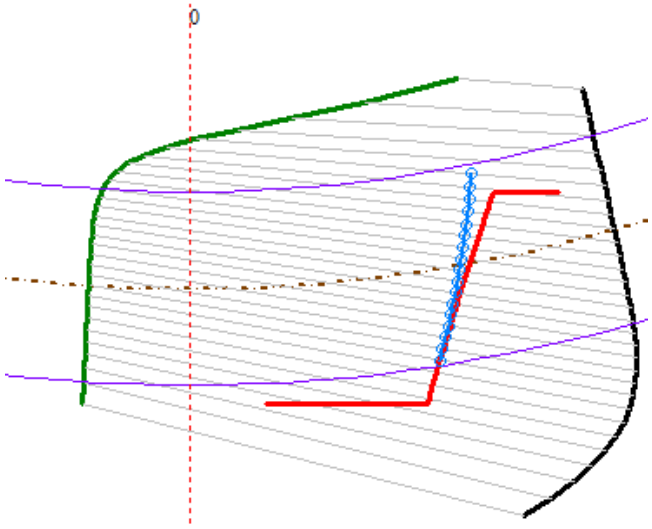

Fig. 5 *Wheel contour (blue) resulting from the hobbing simulation between tooth root and tooth tip (purple) as a sequence of intersection points with minimum distance to the tooth root boundary (green) for each grid line*

In the case of spur gears, it is only necessary to carry out the simulation of the hobbing process in a spur plane of the gear, since the gear contour, apart from the torsion due to the helix angle, does not change over the width of the gear or hardly changes with a clearly defined width crowning. The enveloped wheel contour of a worm gear, on the other hand, has a significant change in shape over the wheel width. For this reason, the hobbing simulation is performed in several parallel sections. In each of these cuts, the 2D cutter contour is required. For this purpose, the contour in the axial section plane of the tool is first determined from the gear data. Predki [3] provides the calculation of the axial section contour for the common flank shape ZA, ZI, ZN, ZC and ZK of worm gears. In addition, the vertical crowning can be included in the form of a parabola according to DIN 3975-1 [4]. By screwing the axial profile geometry around the tool axis, not only the 3D geometry can be derived, but also the 2D contour in the selected parallel sections can be determined.

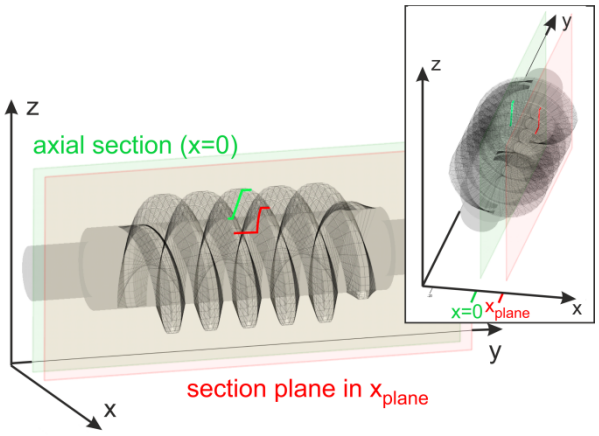

Fig. 6 *3D cutter geometry, axial section profile (green) in axial section plane and calculated tool contour (red) in any section plane.*

Figure 7 shows the calculation algorithm for determining the tool contour in a parallel section plane (yellow) from the axial section plane (x = 0). The contour profile is shown as a red sequence of points. It is possible to determine the coordinates of each point in the plane via an associated screw angle delta. This angle is calculated trigonometrically from the x-coordinate x_{plane} of the plane and the Z-coordinate of the axial section point:

$$\delta = \arcsin\left(\frac{x_{plane}}{z_{plane}}\right) \quad (1)$$

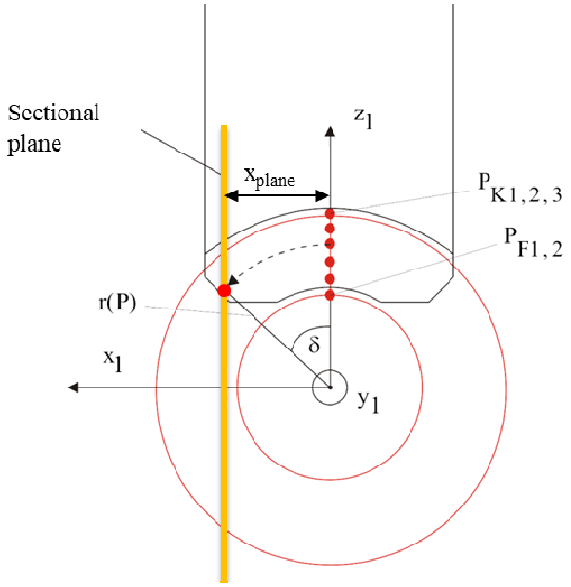

Fig. 7 *Illustration of the determination of the screw angle for determining the tooth contour in a parallel section plane ($x = x_{plane}$) from the axial section plane ($x = 0$)*

In each parallel section, the cutter contour can be calculated in each pitch. With this tool contour, the wheel contour is determined in all parallel section as shown in Figure 5. The separate 2D wheel contours (Fig.8, blue) are combined to form the entire 3D wheel flank. For this purpose, a cubic interpolation is used to generate more grid points over the entire wheel geometry (Fig.8, gray). On the one hand, the number of sections is increased, but also the number of flank points in each of these sections is increased and set to a fixed number. This way, these cuts can be connected and the entire wheel flank is created from the hobbing simulations of each parallel section in detail.

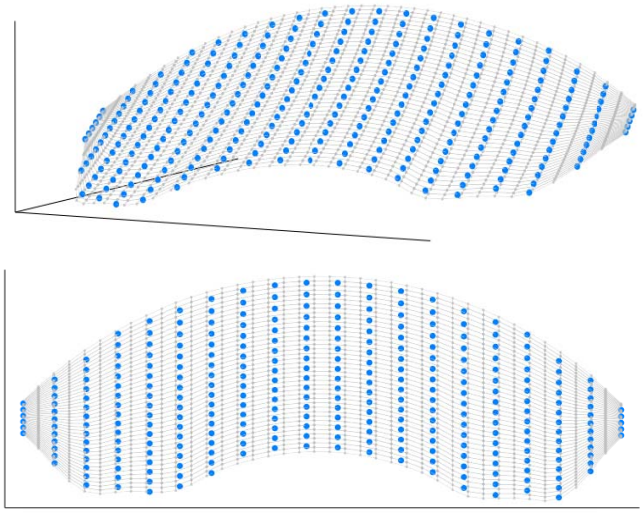

Fig. 8 *Perspective view and radial section of the enveloping wheel contour. The intersection points from the hobbing simulations are gray and the interpolated grid points are blue.*

For illustration purposes, a smaller number of grid lines and section planes as well as interpolation points have been chosen in the figures. To achieve good calculation results, at least 100 grid lines and 30 parallel intersections are selected. The following interpolation is done with at least 40 interpolation sections and 100 points per flank.

For the calculation of the contact pattern, a wheel flank is generated once from the cutter and once from the worm. The wheel flank from the cutter geometry is the real flank before the run-in phase of the worm gear, and the wheel flank from the worm geometry represents the ideal wheel flank after run-in wear. These wheel flanks are rotated towards each other so that they touch at one point.

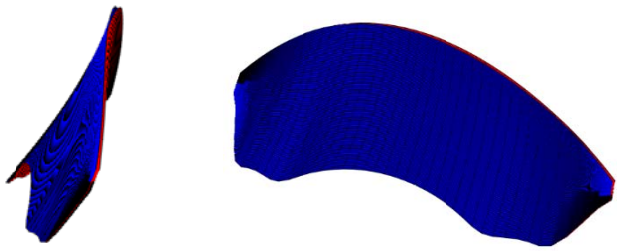

Fig. 9 *Pairing of the two generated enveloping wheel flanks.*

Between all flank points, the distance can be calculated as shown in Figure 10.

$$\text{distance} = \text{radius} \bullet (\alpha_S - \alpha_F) \qquad (2)$$

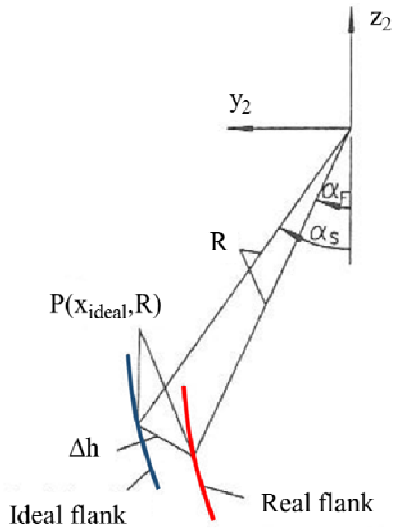

Fig. 10 *Distance calculation between the two wheel flanks*

A contour line diagram is then generated (Fig. 11), on which the flank distance is plotted for each wheel flank coordinate. This contour line diagram is the contact pattern of the gears. It clearly shows where the initial contact zone and consequently the run-in wear will take place. The contact pattern can therefore be used to evaluate how suitable the selected cutter geometry is for generating the wheel flank.

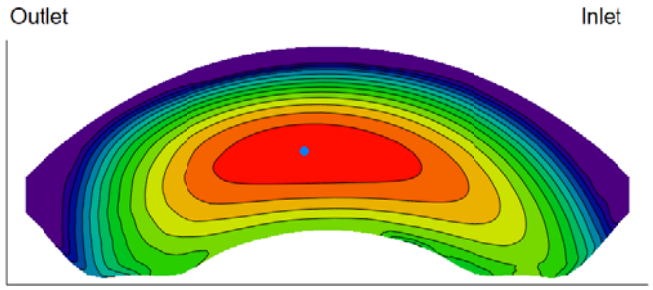

Fig. 11 *Contact pattern – contour line diagram, distance 0 in blue point*

In contrast to the contact pattern, the contact lines are calculated from the flanks actually in contact, which are the wheel flank and the worm flank. The position of the worm flank can be determined from the kinematics of the two gear partners for a given pitch position of the wheel flank. A contact line is automatically set.

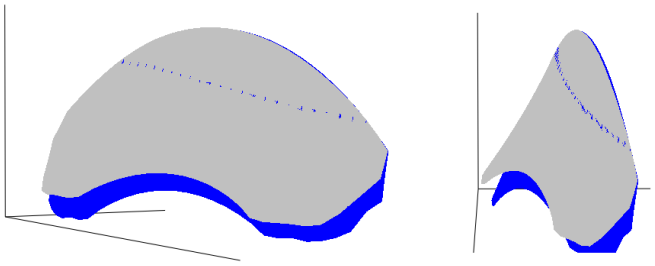

Fig. 12 *Contact line of wheel and worm flank at a specific pitch angle*

In each of the parallel sections of the gear, the point of minimum distance between the flanks is determined. If this point is below a defined limit value, this point counts as a contact point and is part of the contact line. All parallel sections are processed and all found contact points are connected to the contact line. By passing through different pitch positions from the beginning to the end of the tooth contact, the contact line diagrams in the radial section of the worm wheel and in the worm transverse section are obtained.

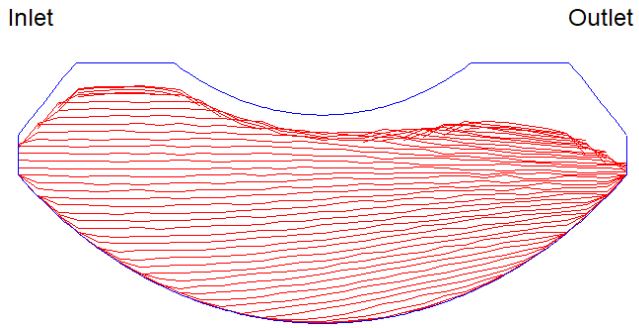

Fig. 13 *Contact lines in the transverse section of the worm*

In addition, the contact lines can be viewed in the top view of the worm. The points that leads to the contact line can also be combined as a meshing line for each parallel section. This allows the length of the contact to be identified.

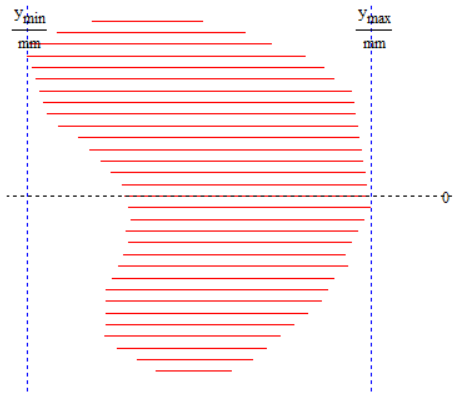

Fig. 14 *Contact lines in the worm face section*

The overlap ε_γ can be determined from minimum (y_{min} = A) and maximum (y_{max} = E) of these mesh lines, which directly indicates the quality of the gearing:

$$\varepsilon_\gamma = \frac{AE}{p_{x1}} = \frac{y_{max} - y_{min}}{p_{x1}} \qquad (3)$$

4. Results and discussion

The developed algorithms were implemented in the software "Trabi 10" at the chair of industrial and automotive drivetrains at Ruhr-University Bochum. This software not only provides the same results for standard gears that can be calculated with existing software, but now also provides results for the mentioned borderline cases (meshing interferences, high number of teeth, etc.). The software is already used in industry and shows a very good fit between theory and practice as can be seen in figure 15.

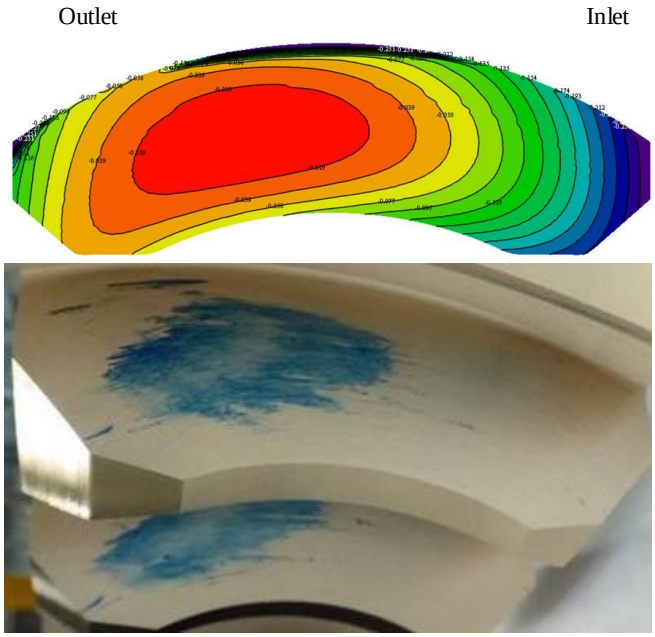

Fig. 15 *Comparison between calculated contact pattern with Trabi 10 (top) and the manufactured contact pattern at "Zahnradfertigung Ott" (bottom)*

5. Conclusion

The software "Trabi 10" with the presented calculation algorithms provides for the first time the possibility to calculate the contact patterns and contact lines of any worm gears without restrictions. Overall, the software is characterized by the fast calculation of many gear variants and the stability of the numerical algorithms. The influence of the various gears and manufacturing parameters on the contact pattern and the contact lines quickly becomes evident and a deep understanding for the correct design of the manufacturing tool is created.

6. References

1. B. Schlecht, *Maschinenelemente 2 Getriebe-Verzahnungen Lagerungen*, Pearson Studium, München (2010)
2. R. Uelpenich, P. Tenberge, *Fast tooth root load capacity optimization based on improved design of hob geometry*, Power Transmissions (2019)
3. W. Predki, *Berechnung von Schneckenflankengeometrien verschiedener Schneckentypen*, Antriebstechnik - Organ der Forschungsvereinigung Antriebstechnik e.V. Heft 2/85, Frankfurt/Main (1985)
4. DIN 3975-1, *Begriffe und Bestimmungsgrößen für Zylinder-Schneckengetriebe mit sich rechtwinklig kreuzenden Achsen-Teil 1: Schnecke und Schneckenrad*, Beuth Verlag, Berlin, (2017)